

**Role of center vortices in Gribov's confinement scenario**

M. Quandt, H. Reinhardt, and G. Burgio

*Institut für Theoretische Physik, Auf der Morgenstelle 14, D-72076 Tübingen Germany*

(Received 21 January 2010; published 16 March 2010)

The connection of Gribov's confinement scenario in the Coulomb gauge with the center vortex picture of confinement is investigated. For this purpose we assume a vacuum wave functional that models the infrared properties of the theory and, in particular, shows strict confinement, i.e. an area law of the Wilson loop. We isolate the center vortex content of this wave functional by standard lattice methods and investigate their contributions to various static propagators of the Hamilton approach to Yang-Mills theory in the Coulomb gauge. We find that the infrared properties of these quantities, in particular, the infrared divergence of the ghost form factor, are dominated by center vortices.

DOI: 10.1103/PhysRevD.81.065016

PACS numbers: 11.15.Ha

**I. INTRODUCTION**

The infrared sector of QCD, in particular, the confinement mechanism, is not fully understood yet, although substantial progress had been made during recent years. The progress comes mainly from lattice calculations [1,2], which gave support to both the dual Meissner effect [3] and the center vortex picture [4] of confinement and also indicate that these two pictures are likely only two sides of the same coin. Furthermore, there is lattice evidence that also Gribov's confinement scenario is triggered by magnetic monopoles and center vortex configurations [5,6]. In addition, one can show analytically that Zwanziger's horizon condition, i.e. an infrared diverging ghost form factor, which is at the heart of Gribov's confinement scenario in the Coulomb gauge, implies dual Meissner effect [7].

In recent years there has been a renewed interest in studying Yang-Mills (YM) theory in the Coulomb gauge, both in the continuum [8] and on the lattice [9–14]. In particular, much work has been devoted to a variational solution of the Yang-Mills Schrödinger equation in the Coulomb gauge [15–23]. Using Gaussian type of Ansatzes for the vacuum wave functional, a set of Dyson-Schwinger equations for the gluon and ghost propagators was derived by minimizing the vacuum energy density. An infrared analysis [22] of these equations exhibits solutions in accord with the Gribov(-Zwanziger) confinement scenario. Imposing Zwanziger's horizon condition one finds an infrared diverging gluon energy and a linear rising static quark (Coulomb) potential [22] and also a perimeter law for the 't Hooft loop [23]. These infrared properties are reproduced by a full numerical solution of the Dyson-Schwinger equations over the entire momentum regime [19], and are also supported by lattice calculations [10,13,14]. Moreover, these lattice calculations also show clear evidence for an infrared divergent ghost form factor

and an infrared suppressed static gluon propagator.<sup>1</sup> While the horizon condition has to be imposed *by hand* in  $D = 3 + 1$ , as there exist also subcritical solutions with an infrared finite ghost form factor<sup>2</sup> [20], the coupled set of Dyson-Schwinger equations in  $D = 2 + 1$  only allows for critical solutions having an infrared diverging ghost form factor [26]. Furthermore, recent studies within the functional renormalization group treatment of the Hamilton approach in the Coulomb gauge yields the horizon condition as a solution of the flow equation [27]. In  $D = 1 + 1$ , finally, the exact ghost form factor is infrared enhanced [21].<sup>3</sup>

Despite the encouraging results for the infrared properties of the various Green's functions (in particular the linear Coulomb potential) and the good agreement of the gluon energy [20] with the lattice data [13,14], the crucial test for the wave functional in the variational approach, namely, the calculation of the Wilson loop, still has to come. In fact, a linear Coulomb potential is necessary but not sufficient for confinement since the Coulomb string tension is only an upper bound to the Wilsonian string tension [8]. With the variational vacuum wave functional at hand it would be, in principle, straightforward to calculate the Wilson loop. However, path ordering makes an

<sup>1</sup>This is different from the Landau gauge, where lattice calculations seem to indicate an infrared finite gluon propagator and ghost dressing function [24], in contradiction to the scaling solution of the Dyson-Schwinger equations [25].

<sup>2</sup>These subcritical solutions are the analogue of the so-called decoupling solution of the Dyson-Schwinger equations in the Landau gauge.

<sup>3</sup>Yang-Mills theory in  $D = 1 + 1$  is nontrivial only on a compact manifold. In the Hamiltonian approach (with a continuous time) space is  $S_1$  so that the momenta are discrete. The zero momentum corresponds to a zero mode of the Faddeev-Popov kernel and is therefore excluded [21].

exact evaluation of the Wilson loop impossible. In Ref. [28] the spatial Wilson loop was calculated from a Dyson equation, which takes care of the path ordering in an approximate fashion, employing the static gluon propagator as input. Despite the rather limited range of applicability of the Dyson equation, a linearly rising potential could be extracted from the obtained Wilson loop.

Here we will proceed along a different line. We assume a wave functional which is known *a priori* to produce an area law for the (spatial) Wilson loop, and calculate with this wave functional the various propagators of the Hamiltonian approach in the Coulomb gauge. The infrared properties of these propagators are then compared with the ones obtained from lattice results in the  $D = 4$  Coulomb gauge which, in turn, agree qualitatively with findings from a Gaussian type of variational wave functional.

A simple choice for a confining wave functional is

$$\Psi[\mathbf{A}] = \mathcal{N} \exp\left(-\frac{1}{8\mu} \int d^3x F_{ij}(\mathbf{x}) F_{ij}(\mathbf{x})\right), \quad (1)$$

where  $F_{ij}$  denotes the spatial components of the non-Abelian field strength and  $\mu$  is a dimensionfull parameter, which, in principle, could serve as variational parameter. We will later see that the scaling properties of  $D = 3$  Yang-Mills theory tie the parameter  $\mu$  to the numerical value of the (spatial) string tension:  $\mu$  thus merely sets the overall scale.

The wave functional in Eq. (1) models the infrared sector of the Yang-Mills vacuum: it is gauge invariant and can be considered as the leading order in a gradient expansion of the true Yang-Mills vacuum wave functional [29]. Furthermore, the functional of Eq. (1) produces an area law for the (spatial) Wilson loop. This is because the  $D = 4$  expectation value of any gauge invariant and  $A_0$ -independent observable  $\Omega[\mathbf{A}]$  in this state is precisely given by the one in the  $D = 3$  dimensional Yang-Mills theory,

$$\langle \Psi | \Omega | \Psi \rangle = \frac{\int \mathcal{D}\mathbf{A} \Omega[\mathbf{A}] \exp\left[-\frac{1}{4\mu} \int d^3x F_{ij}^2(\mathbf{x})\right]}{\int \mathcal{D}\mathbf{A} \exp\left[-\frac{1}{4\mu} \int d^3x F_{ij}^2(\mathbf{x})\right]}. \quad (2)$$

For gauge *variant* observables such as the Green's functions, we need to pick a specific gauge on the vector potential  $\mathbf{A}$ . Choosing the Coulomb gauge  $\nabla \cdot \mathbf{A} = 0$  in  $D = 4$  obviously entails the Landau gauge for the  $D = 3$  YM theory.

The wave functional of Eq. (1) is certainly inappropriate at large momenta where it yields a gluon energy  $\omega(|\mathbf{k}|) \sim |\mathbf{k}|^2$  instead of  $\omega(\mathbf{k}) \sim |\mathbf{k}|$ . However, this should be irrelevant for the confining properties. Also in the deep IR region one does not expect Eq. (1) to exactly reproduce the  $D = 4$  Yang-Mills theory, since the standard lattice gluon and ghost propagator in the  $D = 3$  Landau gauge rather satisfy a decoupling type of solution [24], in contrast to the  $D = 4$  Coulomb gauge [13,14]. Indeed, one would expect the correct wave function to be better described by [30]:

$$\Psi[\mathbf{A}] = \mathcal{N} \exp\left(-\frac{1}{2} \int d^3x F_{ij}(\mathbf{x}) \frac{1}{\sqrt{-D^2 + c}} F_{ij}(\mathbf{x})\right), \quad (3)$$

where  $D^2$  is the adjoint covariant Laplace operator. In Ref. [30], where the  $D = 2 + 1$  theory was examined, the choice  $c = -\lambda_0 + m^2$  was made,  $\lambda_0$  being the lowest eigenvalue of  $-D^2$ . The technical difficulties of working with Eq. (3) are however beyond the scope of this paper, since one does not expect the Laplacian term to modify the vortex content of the  $D = 3$  theory. Even the simplified version given in Eq. (1) cannot be used for analytic calculations; instead, the calculation of expectation values in this state requires conventional three-dimensional Yang-Mills lattice simulations. As stated earlier, these  $D = 3$  lattice calculations must be carried out in the Landau gauge when (1) is used as Schrödinger wave functional in the Coulomb gauge.

The infrared properties of the vacuum sector of the Yang-Mills theory are known to be dominated by center vortices [1]. This is also true in  $D = 3$ . The wave functional Eq. (1) thus contains, among other configurations, an ensemble of percolating center vortices. By standard lattice methods [31] we can extract the center vortex content of this wave functional. Therefore, the use of the wave functional Eq. (1) also allows us to study (on the lattice) how, within the Hamiltonian approach, the Gribov-Zwanziger confinement mechanism is related to the center vortex picture of confinement. Previous lattice calculations [5,6] have shown that removal of center vortices from the (four-dimensional) Yang-Mills ensemble by the method of Ref. [31] makes the ghost form factor infrared finite, analogously to the suppression observed before in the Landau gauge [32]. In the present work we will calculate the center vortex contribution to various Coulomb gauge propagators. The paper is organized as follows:

In the next section, we briefly recall some properties of the  $D = 3$  Yang-Mills theory, in particular, the scaling behavior and some known facts about the Landau gauge Green's functions. Section III contains a description of our numerical setup and the results for the static gluon and ghost form factors in the Coulomb gauge. We also discuss the role of center vortices and their implications for the Gribov-Zwanziger scenario. We close with a brief summary and an outlook on future investigations.

## II. YANG-MILLS THEORY IN THREE DIMENSIONS

Since we want to describe the continuum model of Eq. (1) using a lattice, we must first have a closer look at the scaling properties of the  $D = 3$  YM theory. The lattice model is defined on a  $D = 3$  cubic space-time grid with periodic boundary conditions. We will use the Wilson action and employ various gauge fixing algorithms. The scale  $\mu$  of the continuum wave functional in Eq. (1) plays

the role of the three-dimensional bare YM coupling in the continuum limit,  $\mu = g_0^2$ .

In three-dimensional YM theory, the renormalized coupling  $g_R$  is

$$\beta = \frac{4}{ag_0^2}, \quad g_0^2 = g_R^2[1 + \mathcal{O}(\hbar\beta^{-1})]$$

in terms of the bare coupling  $g_0$  and the lattice spacing  $a$ . The string tension in units of the lattice spacing is therefore

$$\hat{\sigma} \equiv \sigma a^2 = \sigma \frac{16}{\beta^2 g_0^4} = \frac{16\sigma}{\beta^2 g_R^4} + \mathcal{O}(\beta^{-3}). \quad (4)$$

Since  $g_R$  sets the overall scale,  $\sigma/g_R^4$  is a dimensionless constant independent of  $\beta$ , i.e. large Creutz ratios should scale according to

$$\chi(R, R) \approx \hat{\sigma}(\beta) = \frac{\text{const}}{\beta^2} + \mathcal{O}(\beta^{-3}). \quad (5)$$

Large-scale simulations in  $SU(2)$  [33] have indeed confirmed the existence of a scaling window  $\beta \approx 3 \dots 12$  in which the dependency (5) can be observed. More precisely, the best fit [33] is

$$\hat{\sigma}(\beta) = \frac{1.788}{\beta^2} \left( 1 + \frac{1.414}{\beta} + \dots \right) \quad (6)$$

valid for  $\beta \geq 3$ . From Eqs. (4) and (6) and  $\mu = g_0^2$ , we find

$$\frac{\sigma}{\mu^2} = 0.111 \left[ 1 + \frac{1.414}{\beta} + \dots \right], \quad (7)$$

i.e. the variation parameter  $\mu = \mu(\sigma, \beta)$  is fixed once the overall scale  $\sigma$  and the lattice coupling  $\beta$  in the scaling window are given. For the standard value  $\sqrt{\sigma} = 440$  MeV,  $\mu$  falls in the range  $\mu = 1088$  MeV ... 1236 MeV when  $\beta$  is varied in the scaling window. There is however no compelling reason for the string tension of this  $D = 3$  model of the  $D = 4$  Yang-Mills vacuum to coincide with the ‘‘physical’’ string tension of the genuine  $D = 3$  Yang-Mills theory. In view of the following we will then treat  $\mu$  as an adjustable parameter that controls the trade-off between matching the  $D = 4$  string tension or the corresponding Green’s functions.

Ghost and gluon Green’s functions in the Landau gauge are generally expected to be multiplicatively renormalizable, i.e. the lattice data for different  $\beta$  must fall on top of each other once the momentum is expressed in physical units and a finite field renormalization  $Z(\beta)$  is applied. The Gribov-Zwanziger confinement criterion makes qualitative predictions about the deep IR behavior of the Green’s functions. It is based on the idea that the gauge field configurations in the functional integral should be restricted to the so-called fundamental modular region (FMR). The dominant contributions within the FMR should then come from field configurations near the

Gribov horizon, where the near-zero modes of the Faddeev-Popov operator<sup>4</sup>  $M \equiv -\partial\hat{D}$  strongly enhance the Coulomb potential

$$V_c(|\mathbf{x} - \mathbf{y}|) \sim \text{Tr}(M^{-1}(-\Delta)M^{-1}). \quad (8)$$

To enforce the restriction to the FMR, a nonlocal but renormalizable horizon term may be added to the Yang-Mills action. The fact that the partition function is dominated by near-horizon configurations is then expressed as the so-called *horizon condition*, which in turn implies that the ghost propagator should be more singular than the free ghost in the deep infrared,

$$G^{ab}(p) \equiv \langle (M^{-1})^{ab} \rangle = \frac{\delta^{ab}}{p^2} d(p), \quad \lim_{p \rightarrow 0} d^{-1}(p) = 0. \quad (9)$$

Similarly, the gluon propagator should be infrared suppressed or vanishing,

$$D_{\mu\nu}^{ab}(p) \equiv \langle A_\mu^a(-p)A_\nu^b(p) \rangle = \delta^{ab} \left( \delta_{\mu\nu} - \frac{p_\mu p_\nu}{p^2} \right) D(p),$$

$$\lim_{p \rightarrow 0} D(p) < \infty. \quad (10)$$

These results are expected to hold both in  $D = 3$  and  $D = 4$  dimensions. It should be noted, however, that a soft Becchi-Rouet-Stora symmetry breaking but renormalizable mass term is possible in  $D = 3$  and  $D = 4$  which gives rise to the so-called *decoupling solution*. The latter is characterized by a tree-level-like ghost propagator in the IR ( $d(0) = \text{const}$ ) accompanied by an infrared finite, but nonvanishing gluon propagator  $D(0) \neq 0$ . Recent lattice investigations seem to favor this type of behavior in the Landau gauge for both  $D = 3$  and  $D = 4$  which is, however, at odds with both the Gribov-Zwanziger and the Kugo-Ojima criterion favored by functional methods in the continuum. As for the Coulomb gauge in  $D = 4$ , there is, however, ample evidence both from variational methods [17,19] and lattice investigations [13,14] that the ghost propagator is infrared enhanced while the static gluon propagator is infrared vanishing, in accord with the original Gribov scenario.

In the next section, we compute the gluon and ghost Green’s functions in the deep infrared, using the confining wave functional Eq. (1) as a model of the  $D = 4$  ground state in the Coulomb gauge, reliable at least in some intermediate momentum range. Technically, this amounts to a lattice simulation in the  $D = 3$  Landau gauge; in contrast to earlier studies cited above, we will first perform a detour via the maximal center gauge (MCG) to identify the percolating vortex content of each configuration. We can then remove or isolate these vortices before going to

<sup>4</sup>We write  $\hat{D}^{ab} = \partial_\mu + g\hat{A}^{ab} = \partial_\mu - g f^{abc} A_\mu^c$  for the covariant derivative acting on adjoint color fields.

the Landau gauge, and thus study the interplay between the vortex and Gribov-Zwanziger scenario.

### III. NUMERICAL RESULTS

#### A. Numerical setup

Since we are mainly interested in the IR properties we choose in the following a fixed coupling  $\beta = 3.5$  close to the smaller end of the scaling window, which in turn gives access to the smallest momenta while still allowing to extract continuum physics. Calculations were carried out on  $20^3$  and  $40^3$  lattices using a standard over-relaxed version of Creutz' heat-bath algorithm. We employed 500 sweeps for thermalization and 50 to 100 sweeps between measurements to reduce autocorrelations. For each Green's function, we took 300 measurements on the smaller volume  $20^3$ , and 100 measurements for the volume  $40^3$ .

In each measurement, the lattice configuration was first brought to MCG to allow for a clean identification of the center vortex content. The vortices were then either removed or isolated, and both fields (in addition to the unmodified MCG configuration) were subjected to further Landau gauge fixing.<sup>5</sup> As explained above, this corresponds to  $D = 4$  simulations with the trial wave functional Eq. (1) (including its center vortex content) in the Coulomb gauge.

For both gauge fixing steps, we used an iterated over-relaxation algorithm with up to 30 restarts after a random gauge transformation on the initial configuration to reduce the Gribov noise. The gauge fixing procedure was terminated when the local gauge violation was sufficiently small,

$$\|\theta\|_\infty \equiv \max_x \max_{k \in \{1,2,3\}} |\theta^k(x)| < \epsilon = 10^{-12},$$

where in terms of the quaternion representation  $U_\mu = a_\mu^0 + ia_\mu^k \sigma_k$  of the  $SU(2)$  links,

$$\text{MCG: } \theta^k(x) = \frac{1}{2} \sum_{\mu=0}^2 [a_\mu^0(x) a_\mu^k(x) - a_\mu^0(x - \hat{\mu}) a_\mu^k(x - \hat{\mu})],$$

$$\text{Landau: } \theta^k(x) = \frac{1}{2} \sum_{\mu=0}^2 (a_\mu^k(x) - a_\mu^k(x - \hat{\mu})).$$

In all cases, the gauge fixing functional was numerically stationary long before the violation limit was reached.

<sup>5</sup>It should be noted that MCG corresponds to the Landau gauge for the adjoint link, which reduces to the ordinary Landau gauge once the singular vortex background is removed. Thus, the vortex removed MCG configurations *are* already in the Landau gauge. Nevertheless, we have carried out the subsequent Landau gauge fixing step to be sure that we converged to the *best* minimum within our numerical precision.

For the Landau gauge, we further improved the quality of the gauge fixing using either flip preconditioning steps [34] and, on the larger  $40^3$  lattice, simulated annealing methods. However, these improvements had only a marginal effect on the attained maximum of the gauge fixing functional, since the previous MCG fixing acts as a strong preconditioning even when vortices were *not* removed.

#### B. Gluon propagator

The gauge field on the lattice is extracted using the standard definition,

$$a(\beta) A_\mu^k(x + \hat{\mu}/2) \approx \frac{1}{2i} (U_\mu(x) - U_\mu^\dagger(x)) = 2a_\mu^k(x),$$

where  $a(\beta)$  is the lattice spacing and  $U_\mu = a_\mu^0 + ia_\mu^k \sigma_k$  is the quaternion representation of the links.<sup>6</sup> A fast Fourier transformation then gives access to the gluon propagator Eq. (10).<sup>7</sup>

In the left panel of Fig. 1, we first show the  $D = 3$  gluon propagator in the Landau gauge, after prior MCG fixing. As long as vortices are not removed, the resulting propagator is virtually identical with the one obtained by fixing the minimal Landau gauge directly. As can be clearly seen, the removal of vortices has little effect in the UV but clearly suppresses the propagator at intermediate and small momenta.

Figure 2 shows the equal-time gluon propagator  $D_C(\mathbf{p})$  for the Coulomb gauge in  $D = 4$ , as obtained *before* removal of scaling violations. We have compared this data to the  $D = 3$  gluon propagator

- (a) directly in the (minimal) Landau gauge
- (b) in the Landau gauge after prior MCG fixing,
- (c) in the Landau gauge after prior MCG fixing and vortex removal

(The cases *a.* and *b.* are virtually identical, and only *b.* is shown in Fig. 2 to make the plot less cluttered.) The confining  $D = 3$  MCG/Landau propagators  $D_L(p)$  *a.* and *b.* show good agreement in the low and intermediate momentum range with the *naive* instantaneous  $D = 4$  Coulomb propagator, once the (Wilson) string tensions in the two calculations are set equal.<sup>8</sup> (We took  $\sqrt{\sigma} = 440$  MeV to set the scale on the momentum axis.) As expected, the nonconfining Landau gauge propagator

<sup>6</sup>This assumes that the gauge fields are sufficiently smooth and the links close to unity,  $a_\mu^0 \approx 1$ , as ensured by the Landau gauge and the continuum limit.

<sup>7</sup>Since only a single coupling  $\beta = 3.5$  was considered, no further renormalization was necessary. On the smaller lattice, we have verified that all considered ensembles do lead to multiplicatively renormalizable gluon and ghost propagators.

<sup>8</sup>In the UV, we have the expected deviations, since the  $1/p$  behavior of the Coulomb result decays much slower than the  $1/p^2$  typical for the Landau case.



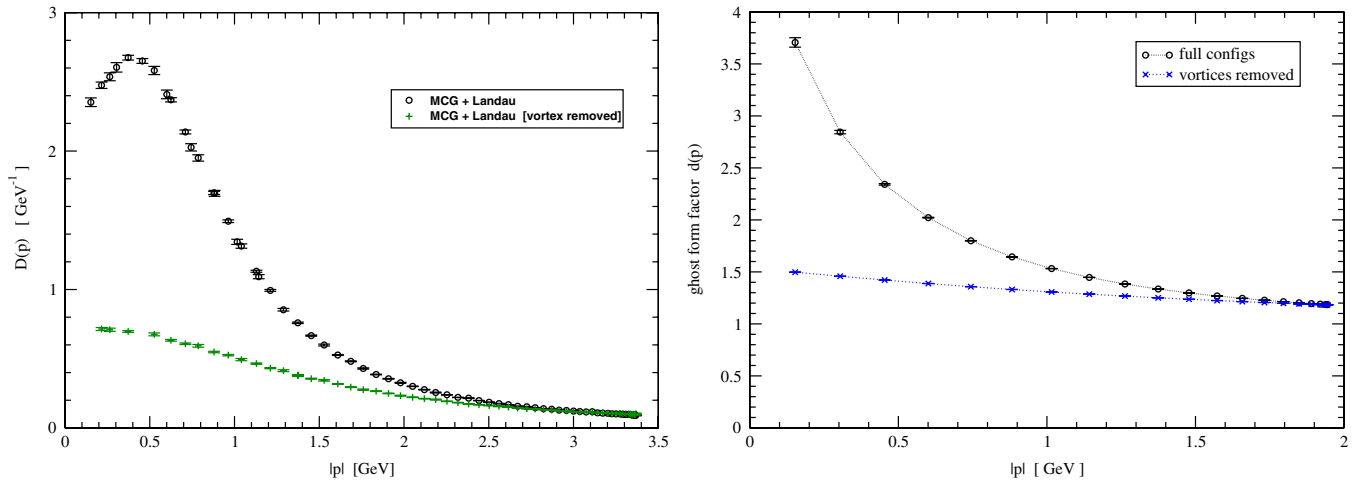


FIG. 1 (color online). Left panel: The  $D = 3$  gluon propagator in the Landau gauge after prior MCG fixing, both with and without vortices. Right panel: The same plot for the  $D = 3$  ghost form factor in the Landau gauge.

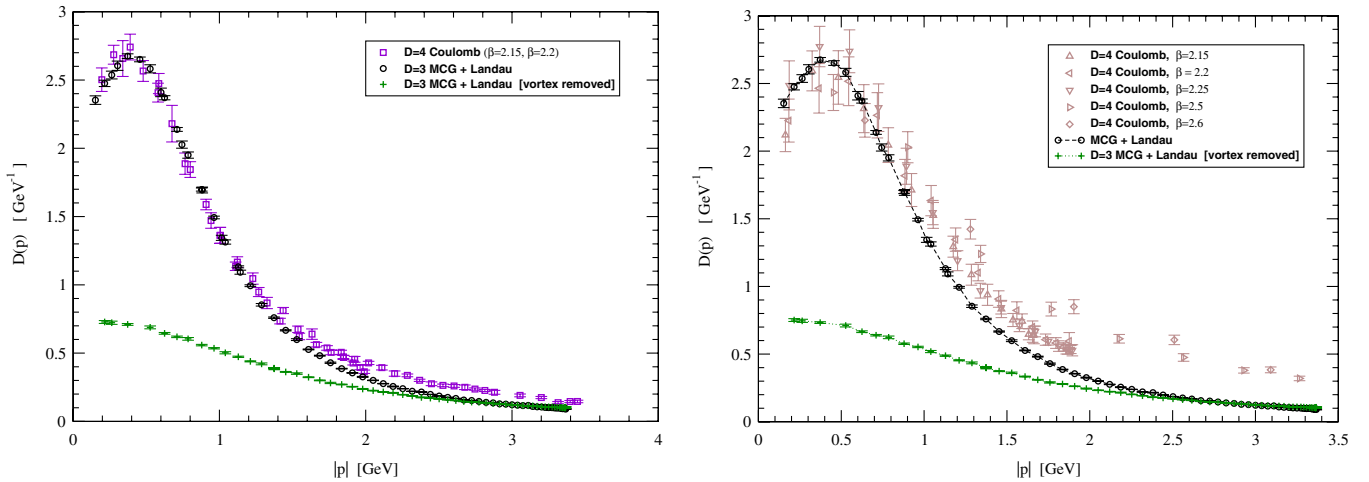


FIG. 2 (color online). The equal-time gluon propagator in the  $D = 4$  Coulomb gauge, compared to the  $D = 3$  gluon propagator in the MCG + Landau gauge, both with and without vortices. In the left panel, we have only included the  $D = 4$  data from two close couplings, which hides the inherent scaling violations. If more couplings are included (right panel), the scaling problems become apparent and the comparison with the  $D = 3$  data is less favorable.

with vortices removed *cannot* be matched with the  $D = 4$  Coulomb data in *any* momentum range.

However, this agreement of the confining propagators must be considered spurious, since the naive  $D = 4$  Coulomb data is subject to severe scaling violations. In Ref. [13], these violations were thoroughly analyzed and a procedure to extract the true instantaneous propagator  $D_C(\mathbf{p})$  in the infinite volume and continuum limit was devised. The result displays proper scaling and the correct deep ultraviolet behavior  $D_C(\mathbf{p}) \sim |\mathbf{p}|^{-1}$ ; it can also be fitted in the entire momentum range through the Gribov formula [13].

As can be seen from the left panel in Fig. 3, the improved static Coulomb propagator  $D_C(\mathbf{p})$  differs considerably from the naive result, so that the spurious agreement with the confining  $D = 3$  ensembles is destroyed. In particular,

the deviation between the strong  $1/p^2$  decay of the  $D = 3$  propagator and the slow  $1/|\mathbf{p}|$  decay of  $D_C(\mathbf{p})$  is now much more apparent. Qualitative agreement in the phenomenologically important momentum range around 1 GeV can only be reached if the  $D = 3$  momentum is scaled with a factor  $\sim 2.5$  as compared to the  $D = 4$  case (see right panel in Fig. 3). This in turn would mean that the scale parameter  $\mu$  in the initial wave functional Eq. (1) must be altered by the same factor and the  $D = 3$  string tension would no longer match the  $D = 4$  result.<sup>9</sup> The best agreement is

<sup>9</sup>In the very deep IR, the  $D = 3$  and  $D = 4$  propagators cannot be matched even with the relaxed condition on  $\mu$ , since the correct  $D = 4$  static Coulomb propagator vanishes as  $|\mathbf{p}| \rightarrow 0$ , while the  $D = 3$  MCG-Landau propagator  $D_L(p)$  goes to a nonzero value in this limit.

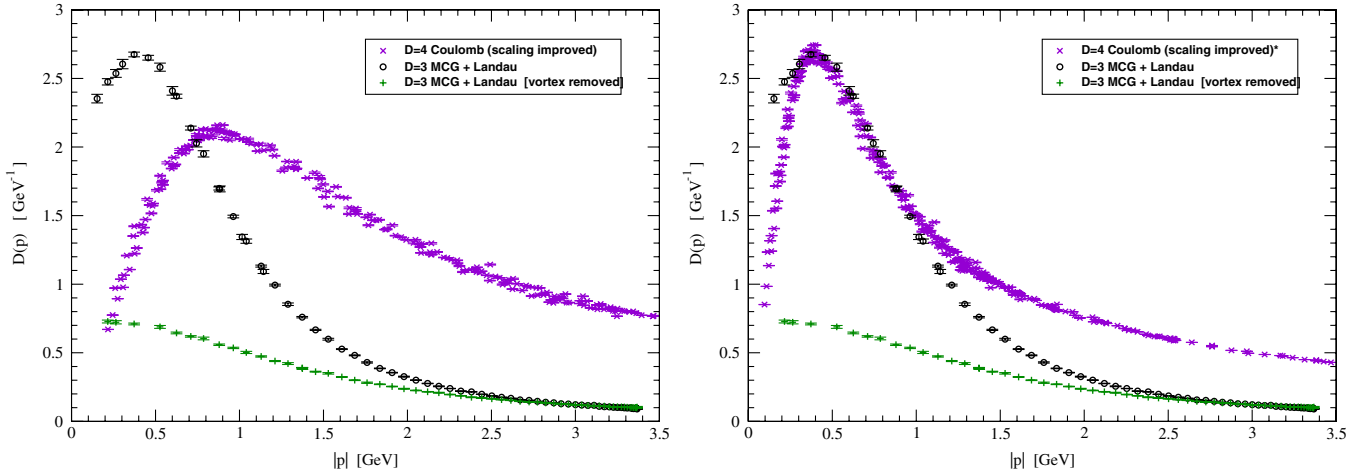


FIG. 3 (color online). The equal-time gluon propagator in the  $D = 4$  Coulomb gauge, compared to the  $D = 3$  gluon propagator in the MCG + Landau gauge, both with and without vortices. The scaling violations in the Coulomb data are removed [13] to exhibit the true continuum result. In the left panel, the (Wilson) string tension of the  $D = 3$  and  $D = 4$  calculations are matched, while the right panel has  $\sigma_{3D} \approx 6.2\sigma_{4D}$ . (For simplicity, we have scaled  $\sigma_{4D}$  and left  $\sigma_{3D}$  at the standard value.)

thus obtained if  $\sigma_{3D} \approx 6.2\sigma_{4D}$ , corresponding to  $\mu \approx 7$  GeV.

The vortex-removed ensemble  $d$  leads to a gluon propagator which is incompatible with the  $D = 4$  Coulomb result in *any* momentum range, even if the restrictions on the parameter  $\mu$  are relaxed. This shows that the percolating center vortex content is not only indispensable for the confining properties of the Wilson loop, but also for the qualitative behavior of the gluon propagator at intermediate momenta.

As stated above, a better approximation of the correct vacuum wave functional is given by Eq. (3). Indeed, either by inspecting Fig. 3 or on simple dimensional arguments, it should be clear that one should rather compare the  $D = 4$  static Coulomb propagator  $D_C(\mathbf{p})$  with  $pD_L(p)$  [14], which

on the other hand will mimic the somewhat less crude approximation of the vacuum wave functional:

$$\Psi[\mathbf{A}] = \mathcal{N} \exp\left(-\frac{1}{2} \int d^3x F_{ij}(\mathbf{x}) \frac{1}{\sqrt{-\nabla^2}} F_{ij}(\mathbf{x})\right). \quad (11)$$

The data basically coincide when tuning  $\sigma_{3D} \approx 1.49\sigma_{4D}$ , as can be seen in Fig. 4. Such good agreement in the direction of the wave functional given in Eq. (3) definitely deserves further investigation.

### C. The ghost form factor

Although large volume simulations performed in a setup similar to ours clearly show a decoupling behavior also for the Landau ghost in  $D = 3$  [24], for the momenta available in our simulations this regime still has not kicked in, so that Eq. (1) might still be considered a valid approximation in the following. Future simulations closer to the thermodynamic/continuum limit will however explicitly have to deal with Eq. (3) or at least Eq. (11), since the simple dimensional argument leading for the static gluon to the comparison in Fig. 4 cannot obviously be applied to the Faddeev-Popov operator.

The right panel of Fig. 1 shows the dimensionless ghost form factor (9) as obtained from the  $D = 3$  Landau gauge with prior MCG fixing. Without vortex removal, the result is virtually identical to the direct Landau gauge fixing, and a power law behavior of the form

$$d(p) \sim p^{-2\kappa}, \quad \kappa = 0.23(1) \quad (12)$$

can be fitted. This agrees well with the infrared exponent of the  $D = 4$  Coulomb gauge [10], which is not subject to scaling violations. Figure 5 compares the ghost form factors in the  $D = 3$  Landau gauge and the  $D = 4$  Coulomb gauge quantitatively; as expected from the matching IR

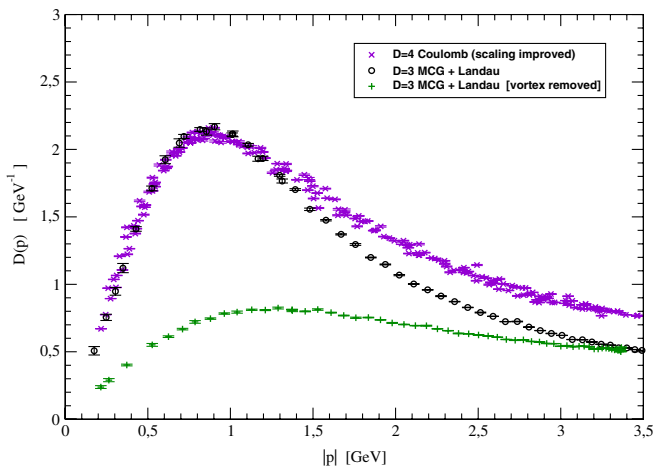


FIG. 4 (color online). The gluon static propagator in the  $D = 4$  Coulomb gauge, compared to the approximation  $pD_L(p)$  of Eq. (11) in the  $D = 3$  MCG + Landau gauge.

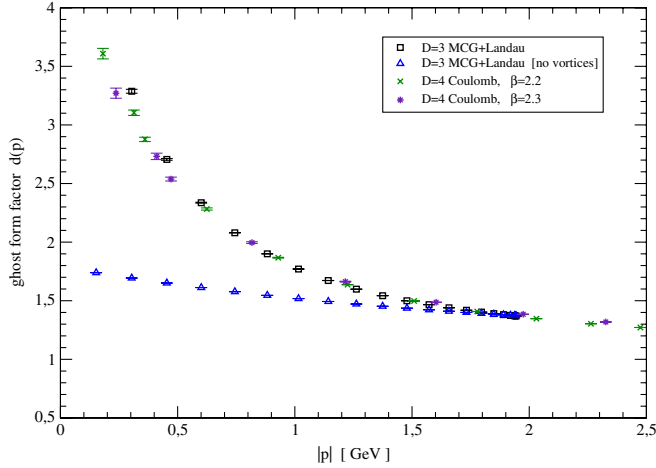


FIG. 5 (color online). The ghost form factor in the  $D = 4$  Coulomb gauge, compared to the same quantity in the  $D = 3$  MCG + Landau gauge. The  $D = 4$  data is from a  $32^4$  lattice at  $\beta = 2.2$  and  $\beta = 2.3$ , while the  $D = 3$  data was obtained on  $40^3$  lattices with  $\beta = 3.5$ .

exponent, the comparison is fairly good. In the UV,  $d(p)$  approaches 1 in both  $D = 3$  and  $D = 4$ , so the qualitative agreement is also good in this regime. (A closer comparison of possible anomalous dimensions in the subleading terms is beyond our current numerical precision.)

It should be noted that the powerlike behavior Eq. (12) is conformally invariant, i.e. the exponent  $\kappa$  is not affected by any rescaling of the momenta or string tension. This allows to maintain the good agreement of the ghost form factor, while relaxing the condition on  $\mu$  to make the gluon propagators match (approximately). With the higher value of  $\mu$  and the three-dimensional string tension, it is therefore possible to reproduce at least qualitatively both the gluon and ghost form factor from the wave functional Eq. (1), at least in the intermediate momentum range.

From the right panel in Fig. 1, it is also seen that the vortex-removed ghost form factor in  $D = 3$  is virtually flat ( $\kappa < 0.05$ ) so that it cannot be matched even qualitatively to the  $D = 4$  Coulomb result. In particular, it seems impossible to satisfy the horizon condition  $d(0)^{-1} = 0$  once center vortices are removed. This is, of course, expected

since vortices live on the Gribov horizon and are thus indispensable to maintain enough near-zero modes of the Faddeev-Popov operator to produce the diverging ghost form factor. A similar conclusion was also reached in Ref. [6] from the direct study of the low-lying Faddeev-Popov spectrum.

#### IV. CONCLUSION AND OUTLOOK

In this paper we have investigated the properties of the static propagators of the Hamiltonian approach in the Coulomb gauge, assuming the wave functional Eq. (1), which shows strict confinement, as an approximation of the low energy limit of the true Yang-Mills vacuum wave functional. The calculation of expectation values of observables in the  $D = 3 + 1$  Hamiltonian approach in the Coulomb gauge in this state requires an ordinary  $D = 3$  lattice simulation in the Landau gauge. Adjusting the free scale  $\mu$  of the state Eq. (1) yields propagators which in a low to intermediate momentum regime (up to about 1 GeV) reproduce quite well the exact lattice propagators of the  $D = 3 + 1$  Coulomb gauge, which also agree qualitatively with propagators obtained in the variational approach to continuum Yang-Mills theory in the Coulomb gauge. An even better agreement should be obtained by employing the wave functional given in Eq. (3) and (11), as Fig. 4 shows.

The propagators drastically change in the infrared when the magnetic center vortices occurring with the weight  $|\Psi[\mathbf{A}]|^2$  in the wave functional are removed by the method of Ref. [31]. In particular, the ghost form factor loses its infrared singularity and the horizon condition is no longer satisfied. These results indicate that there is no need to include additional explicit center vortex degrees of freedom in the trial wave functional of the variational approach, as was proposed recently [35].

#### ACKNOWLEDGMENTS

We would like to thank J. Greensite for his careful reading of the manuscript and useful suggestions. This work was partly supported by DFG under Contract No. DFG-Re856/6-3.

[1] For lattice evidence for the center vortex picture of confinement see: L. Del Debbio, M. Faber, J. Greensite, and S. Olejnik, Phys. Rev. D **55**, 2298 (1997); K. Langfeld, H. Reinhardt, and O. Tennert, Phys. Lett. B **419**, 317 (1998); M. Engelhardt, K. Langfeld, H. Reinhardt, and O. Tennert, Phys. Rev. D **61**, 054504 (2000); J. Greensite, Prog. Part. Nucl. Phys. **51**, 1 (2003).

[2] For lattice evidence for the dual superconductor picture of confinement see A. S. Kronfeld, G. Schierholz, and U.-J. Wiese, Phys. Lett. B **198**, 516 (1987); T. Suzuki and I. Yotsuyanagi, Phys. Rev. D **42**, 4257 (1990); S. Hoki *et al.*, Phys. Lett. B **272**, 326 (1991); G. Bali, Ch. Schlichter, and K. Schilling, Prog. Theor. Phys. Suppl. **131**, 645 (1998) and Ref. therein.

- [3] Y. Nambu, Phys. Rev. D **10**, 4262 (1974); S. Mandelstam, Phys. Lett. **53B**, 476 (1975); G. Parisi, Phys. Rev. D **11**, 970 (1975); Z. F. Ezawa and H. C. Tze, Nucl. Phys. **B100**, 1 (1975); R. Brout, F. Englert, and W. Fischler, Phys. Rev. Lett. **36**, 649 (1976); F. Englert and P. Windey, Nucl. Phys. **B135**, 529 (1978); G. 't Hooft, Nucl. Phys. **B190**, 455 (1981); Phys. Scr. **25**, 133 (1982).
- [4] G. 't Hooft, Nucl. Phys. **B138**, 1 (1978); G. Mack and V. B. Petkova, Ann. Phys. (N.Y.) **123**, 442 (1979); G. Mack, Phys. Rev. Lett. **45**, 1378 (1980); G. Mack and V. B. Petkova, Ann. Phys. (N.Y.) **125**, 117 (1980); G. Mack, and E. Pietarinen, Nucl. Phys. **B205**, 141 (1982); Y. Aharonov, A. Casher, and S. Yankielowicz, Nucl. Phys. **B146**, 256 (1978); J. M. Cornwall, Nucl. Phys. **B157**, 392 (1979); H. B. Nielsen and P. Olesen, Nucl. Phys. **B160**, 380 (1979); J. Ambjorn and P. Olesen, Nucl. Phys. **B170**, 60 (1980); E. T. Tomboulis, Phys. Rev. D **23**, 2371 (1981).
- [5] J. Greensite and S. Olejnik, Phys. Rev. D **67**, 094503 (2003).
- [6] J. Greensite, S. Olejnik, and D. Zwanziger, J. High Energy Phys. 05 (2005) 070.
- [7] H. Reinhardt, Phys. Rev. Lett. **101**, 061602 (2008).
- [8] D. Zwanziger, Phys. Rev. Lett. **90**, 102001 (2003).
- [9] K. Langfeld and L. Moyaerts, Phys. Rev. D **70**, 074507 (2004).
- [10] M. Quandt, G. Burgio, S. Chimchinda, and H. Reinhardt, Proc. Sci., LAT2007 (2007) 325.
- [11] A. Voigt, M. Ilgenfritz, M. Müller-Preussker, and A. Sternbeck, Proc. Sci., LAT2007 (2007) 338.
- [12] A. Voigt, M. Ilgenfritz, M. Müller-Preussker, and A. Sternbeck, Phys. Rev. D **78**, 014501 (2008).
- [13] G. Burgio, M. Quandt, and H. Reinhardt, Phys. Rev. Lett. **102**, 032002 (2009).
- [14] G. Burgio, M. Quandt, and H. Reinhardt, arXiv:0911.5101.
- [15] A. P. Szczepaniak and E. S. Swanson, Phys. Rev. D **65**, 025012 (2001).
- [16] C. Feuchter and H. Reinhardt, Phys. Rev. D **70**, 105021 (2004).
- [17] C. Feuchter and H. Reinhardt, arXiv:hep-th/0402106.
- [18] H. Reinhardt and C. Feuchter, Phys. Rev. D **71**, 105002 (2005).
- [19] D. Epple, H. Reinhardt, and W. Schleifenbaum, Phys. Rev. D **75**, 045011 (2007).
- [20] D. Epple, H. Reinhardt, W. Schleifenbaum, and A. P. Szczepaniak, Phys. Rev. D **77**, 085007 (2008).
- [21] H. Reinhardt and W. Schleifenbaum, Ann. Phys. (N.Y.) **324**, 735 (2009).
- [22] W. Schleifenbaum, M. Leder, and H. Reinhardt, Phys. Rev. D **73**, 125019 (2006).
- [23] H. Reinhardt and D. Epple, Phys. Rev. D **76**, 065015 (2007).
- [24] A. Cucchieri and T. Mendes, Phys. Rev. D **78**, 094503 (2008); Phys. Rev. Lett. **100**, 241601 (2008); I. L. Bogolubsky *et al.*, Proc. Sci., LATTICE2009 (2009) 237.
- [25] L. v. Smekal, R. Alkofer, and A. Hauck, Phys. Rev. Lett. **79**, 3591 (1997); C. Fischer and J. Pawłowski, Phys. Rev. D **75**, 025012 (2007); C. Fischer, A. Maas, and J. Pawłowski, Ann. Phys. (N.Y.) **324** 2408 (2009).
- [26] C. Feuchter and H. Reinhardt, Phys. Rev. D **77**, 085023 (2008).
- [27] M. Leder, J. Pawłowski, A. Weber, and H. Reinhardt (to be published).
- [28] M. Pak and H. Reinhardt, Phys. Rev. D **80**, 125022 (2009).
- [29] J. Greensite, Nucl. Phys. **B158**, 469 (1979).
- [30] J. Greensite and S. Olejnik, Phys. Rev. D **77**, 065003 (2008).
- [31] P. de Forcrand and M. D'Elia, Phys. Rev. Lett. **82**, 4582 (1999).
- [32] J. Gattnar, K. Langfeld, and H. Reinhardt, Phys. Rev. Lett. **93**, 061601 (2004). K. Langfeld, G. Schulze, and H. Reinhardt, Phys. Rev. Lett. **95**, 221601 (2005).
- [33] M. J. Teper, Phys. Rev. D **59**, 014512 (1998).
- [34] I. L. Bogolubsky *et al.*, Phys. Rev. D **74**, 034503 (2006); **77**, 014504 (2008).
- [35] A. Szczepaniak (private communication).